Energetics and Mechanism of the Thermal Decarboxylation of (CO)$_4$FeCOOH$^-$ in the Gas Phase

L. S. Sunderlin and Robert R. Squires*

Contribution from the Department of Chemistry, Purdue University, West Lafayette, Indiana 47907. Received August 20, 1992

Abstract: The energetics and mechanism of decarboxylation of (CO)$_4$FeCOOH$^-$ to form CO$_2$ and (CO)$_4$FeH$^-$, a key step in the Fe(CO)$_5$-catalyzed water-gas shift reaction, is investigated using the flowing afterglow-triple quadrupole technique. Previous studies of collisional activation of (CO)$_4$FeCOOH$^-$ in the gas phase showed only loss of CO ligands, suggesting that base catalysis is necessary for decarboxylation. We have now observed gas-phase decarboxylation of this hydroxycarbonyl ion using energy-resolved collision-induced dissociation. Decarboxylation competes with decarbonylation at translational energies near the reaction threshold, indicating that unimolecular β-elimination of CO$_2$ can occur. Loss of two carbonyl ligands to form (CO)$_3$FeOH$^-$ is the dominant process at somewhat higher energies. The thresholds for loss of CO, 2CO, and CO$_2$ are 21.4 ± 3.9, 30.2 ± 2.8, and 18.9 ± 3.2 kcal/mol, respectively. The latter number corresponds to a barrier for an exothermic reaction. DH[Fe(CO)$_5$–OH$^-$] = 60.8 ± 3.4 kcal/mol is determined by measurement of the equilibrium constant for hydroxide exchange between Fe(CO)$_5$ and SO$_2$. (CO)$_4$FeSOOH$^-$ + CO$_2$ is formed as a side product of this reaction, and the structure of this species is investigated. These data are combined with other thermochemistry to derive a model reaction–energy profile for the Fe(CO)$_5$-catalyzed water-gas shift reaction.

Introduction

One of the key strengths of gas-phase ion chemistry is the opportunity it affords to examine the intrinsic properties of reactive chemical intermediates. These studies can provide information about the structures, stability, and kinetic behavior of transient species that is difficult or impossible to obtain from traditional condensed-phase experiments. In organic chemistry, gas-phase ion studies have made numerous contributions to our current understanding of the intrinsic properties and reactivity of carbocations, carbanions, radicals, and carbenes.[1] Transition-metal organometallic chemistry also possesses a rich variety of reactive intermediates such as coordinatively unsaturated metal complexes and radicals for which useful new chemical and physical information has been obtained through gas-phase ion research.[2,3]

Some time ago, we reported the formation and chemical characterization of (CO)$_4$FeCOOH$^-$ (I) in the gas phase.[4] This particular organometallic anion is proposed as a reactive inter-
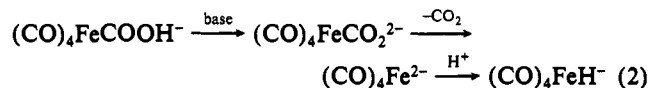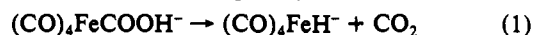

I
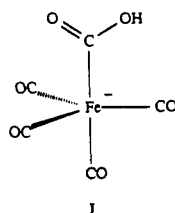
mediate in the Fe(CO)$_5$-catalyzed water-gas shift (WGS) reaction[5–10] in alkaline solution, and it is representative of the general

Scheme I

NET:　H$_2$O　+　CO　⟶　H$_2$　+　CO$_2$
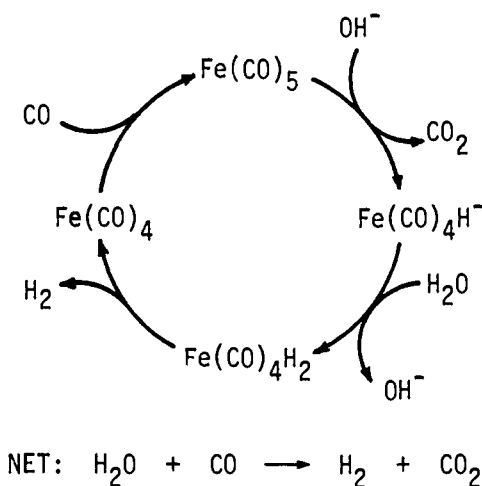
class of metal hydroxycarbonyl (metallocarboxylic acid) complexes. Although Fe(CO)$_5$ in aqueous, alkaline solution is not a practical catalyst for the WGS reaction, it serves as a convenient paradigm for mechanistic studies. The general catalytic cycle for Fe(CO)$_5$ (Scheme I)[5,7] is believed to involve nucleophilic activation of CO followed by decarboxylation of the transient (CO)$_4$FeCOOH$^-$ to form CO$_2$ and the metal hydride (CO)$_4$FeH$^-$. Previous studies in solution suggested that CO$_2$ loss from 1 proceeds either through unimolecular β-elimination,[6,7,11] reaction 1, or a reaction involving base catalysis,[8] as shown in reaction 2. Both mechanisms have been demonstrated in analogous systems.[5,12]

$$(CO)_4FeCOOH^- \rightarrow (CO)_4FeH^- + CO_2 \qquad (1)$$

$$(CO)_4FeCOOH^- \xrightarrow{\text{base}} (CO)_4FeCO_2^{2-} \xrightarrow{-CO_2}$$
$$(CO)_4Fe^{2-} \xrightarrow{H^+} (CO)_4FeH^- \qquad (2)$$

(1) Nibbering, N. M. M. *Adv. Phys. Org. Chem.* **1988**, *24*, 1–55. Bowie, J. H. *Mass Spectrom.* **1985**, *8*, 161. DePuy, C. H.; Bierbaum, V. M. *Acc. Chem. Res.* **1981**, *14*, 146. Hammerum, S. *Mass Spectrom. Rev.* **1988**, *7*, 123. Pellerite, M. J.; Brauman, J. I. In *Comprehensive Carbanion Chemistry, Part A*; Buncel, E., Durst, T., Eds.; Elsevier: Amsterdam, 1980. *Gas Phase Ion Chemistry*; Bowers, M. T., Ed.; Academic: New York, 1979–1984; Vols. 1–3. Lammertsma, K.; Schleyer, P. v. R.; Schwarz, H. *Angew. Chem., Int. Ed. Engl.* **1989**, *28*, 1321–1339.

(2) Squires, R. R. *Chem. Rev.* **1987**, *87*, 623–646.

(3) *Gas Phase Inorganic Chemistry*; Russell, D. H., Ed.; Plenum Press: New York, 1989. Eller, K.; Schwarz, H. *Chem. Rev.* **1991**, *91*, 1121–1177. *Energetics of Organometallic Species*; Simoes, J. A. M., Ed.; Kluwer: Dordrecht, 1992.

(4) Lane, K. R.; Lee, R. E.; Sallans, L.; Squires, R. R. *J. Am. Chem. Soc.* **1984**, *106*, 5767–5772.

(5) For an extensive review see: Ford, P. C.; Rokicki, A. *Adv. Organomet. Chem.* **1988**, *28*, 139–217.

(6) (a) Ford, P. C.; Ungermann, C.; Landis, V.; Moya, S. A.; Rinker, R. C.; Laine, R. M. *Adv. Chem. Ser.* **1978**, *173*, 81–93. (b) Ford, P. C. *Acc. Chem. Res.* **1981**, *14*, 31–37. (c) Trautman, R. J.; Gross, D. C.; Ford, P. C. *J. Am. Chem. Soc.* **1985**, *107*, 585–593. (d) Trautman, R. J.; Gross, D. C.; Ford, P. C. *J. Am. Chem. Soc.* **1985**, *107*, 2355–2362.

(7) Kang, H. C.; Mauldin, C. H.; Cole, T.; Slegeir, W.; Cann, K.; Pettit, R. *J. Am. Chem. Soc.* **1977**, *99*, 8323–8325. Grice, N.; Kao, S. C.; Pettit, R. *J. Am. Chem. Soc.* **1979**, *101*, 1627–1628. Pettit, R.; Cann, K.; Cole, T.; Mauldin, C. H.; Slegeir, W. *Adv. Chem. Ser.* **1978**, *173*, 121–130.

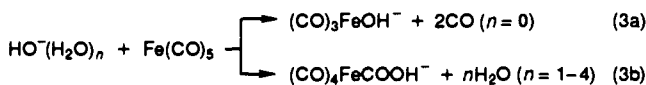(8) Pearson, R. G.; Mauermann, H. *J. Am. Chem. Soc.* **1982**, *104*, 500–504.

(9) Bennett, M. A. *J. Mol. Catal.* **1987**, *41*, 1–20.

(10) King, A. D.; King, R. B.; Yang, D. B. *J. Am. Chem. Soc.* **1980**, *102*, 1028–1032.

(11) Frazier, C. C.; Hanes, R. M.; King, A. D.; King, R. B. *Adv. Chem. Ser.* **1978**, *173*, 94–105. King, A. D.; King, R. B.; Yang, D. B. *J. Am. Chem. Soc.* **1981**, *103*, 2699–2704.

In earlier flowing afterglow studies[4,13] we were able to generate I as a stable, long-lived species in the gas phase from reactions of partially hydrated hydroxide ions with $Fe(CO)_5$, reaction 3.

$$HO^-(H_2O)_n + Fe(CO)_5 \begin{cases} \longrightarrow (CO)_3FeOH^- + 2CO \ (n = 0) & (3a) \\ \longrightarrow (CO)_4FeCOOH^- + nH_2O \ (n = 1-4) & (3b) \end{cases}$$

Estimates of the absolute heats of formation of I and the iron hydride complex $(CO)_4FeH^-$ suggested that the decarboxylation is exothermic, implying that a barrier for unimolecular β-elimination of CO_2 from I must exist. Collision-induced dissociation (CID) of I in a prototype flowing afterglow-triple quadrupole instrument failed to show $(CO)_nFeH^-$ ($n \leq 4$) fragments derived from CO_2 loss; instead only sequential CO-ligand dissociation was observed. In view of the known behavior of metal hydroxycarbonyl complexes in solution,[5] the absence of decarboxylation from I was somewhat surprising. This result was taken to mean that the barrier for CO_2 loss exceeded that for CO loss and, further, that decarboxylation of I in solution probably proceeds by a base-catalyzed mechanism.

In this paper we present a detailed investigation of the unimolecular reactions of $(CO)_4FeCOOH^-$ using improved analytical procedures that clearly show decarboxylation as a low-energy, but inefficient, process. Quantitative studies of the collision energy dependence of selected dissociation reactions of I are combined with new measurements of its absolute heat of formation to construct a gas-phase thermochemical profile for the model catalytic cycle proposed for the WGS reaction.

Experimental Section

All experiments were performed with a flowing afterglow–triple quadrupole apparatus described previously.[14] The standard operating conditions in the 7.6 cm i.d. × 100 cm tube were $P(He) = 0.40$ Torr, $F(He) = 190$ STP cm^3/s, and $T = 298$ K. OH^- was generated by electron impact on N_2O to produce O^-, followed by hydrogen atom abstraction from CH_4. Hydrated hydroxide ions $HO^-(H_2O)_n$ were formed by addition to the flow tube of either pure H_2O vapor or the head vapors from a tetrahydrofuran/H_2O mixture.[4] The resulting cluster ions react rapidly with $Fe(CO)_5$ to produce I, reaction 3.[15] A convenient alternative procedure for generating I was also employed in which $HOCO_2^-$ is first formed from reaction of HO^- with excess CO_2 added in the upstream portion of the flow tube. Reaction of $HOCO_2^-$ with $Fe(CO)_5$ then produces I by OH^- transfer. Bisulfite ions were similarly produced from reaction of $HOCO_2^-$ with SO_2.[16]

Ions are thermalized by ca. 10^5 collisions with the helium bath gas in the flow tube and then gently extracted through a 1-mm orifice and focused into the Extrel triple quadrupole mass analyzer. The desired reactant ion is selected with the first quadrupole and injected into the rf-only, gas-tight central quadrupole (Q2) with an axial kinetic energy determined by the Q2-rod offset voltage. Argon collision gas is maintained in Q2 at a pressure of ≤ 0.04 mTorr, ensuring that secondary collisions will be negligible. Fragment ions resulting from CID are efficiently contained in Q2 and extracted by a low voltage exit lens into the third quadrupole, which is maintained at a constant attractive voltage (5–10 V) with respect to the variable Q2-rod voltage. Ion detection is carried out with a conversion dynode and an electron multiplier operating in pulse-counting mode.

He (99.995%) and Ar (99.995%) were obtained from Airco, CH_4 (99%), N_2O (99%), and SO_2 (99.98%) were obtained from Matheson, and $Fe(CO)_5$ (99.5%) was obtained from Alfa and used as received except for freeze–pump–thawing prior to use.

Reaction Rate Measurements. Bimolecular ion–molecule reaction rates were measured under pseudo-first-order conditions using standard techniques.[4,14,17] Ion abundances were monitored as a function of the neutral reagent flow rate through ring inlets located in the flow tube at

effective reaction distances of 38, 48, and 63 cm. The flow rates were determined from the change in total pressure with time when the reagent flow was diverted from the flow tube into a calibrated volume. The estimated accuracy of the measurements is ±30% for the reactions discussed in this paper. These error limits are somewhat larger than the usual ±20%[18] because of the limited reactant ion depletion (less than one order of magnitude) achievable with reversible reactions. Branching ratios measured as a function of reaction distance are extrapolated to zero reaction distance in order to account for differential ion diffusion and secondary ion–molecule reactions. These effects limit the accuracy of the measured branching ratios in this experiment to ±50%.

CID Threshold Measurement and Analysis. The data collection and analysis procedures for obtaining CID threshold energies with the flowing afterglow-triple quadruple instrument are described in detail elsewhere.[19] Briefly, the axial kinetic energy of the mass-selected reactant ion is scanned while the intensity of the CID fragment ion formed in Q2 under single-collision conditions is monitored. The center-of-mass collision energy for the system is given by $E_{CM} = E_{lab}[m/(M + m)]$, where E_{lab} is the nominal lab energy as determined by the Q2-rod offset voltage and M and m represent the masses of the reactant ion and neutral target, respectively. The energy axis origin is verified by retarding potential analysis with Q2 serving as the retarding field element. The reactant ion kinetic energy distribution, as given by the first derivative of the retarding curve, has a near-Gaussian shape with a full-width at half-maximum of 0.5–2 eV (lab frame). Absolute cross sections are calculated by use of $\sigma_p = I_p/INl$, where σ_p is the cross section for a particular product, I_p is the intensity of the product (counts/sec), N is the number density of the neutral reagent, l is the effective path length for reaction (24 ± 4 cm), and I is the intensity of the reactant ion beam.[19,20] This is accurate as long as the extent of conversion of reactant ions to products remains low (<ca. 5%). The argon target pressure in Q2 (≤ 0.04 mTorr) is low enough to ensure predominantly single collision conditions. Different collection or detection efficiencies for the reactant and product ions are the main source of inaccuracies in the absolute cross sections, which have an estimated uncertainty of a factor of 2.

A plot of the product ion yield or dissociation cross section versus the center-of-mass collision energy gives rise to an ion appearance function from which the activation energy for the dissociation may be deconvoluted. The shape of the appearance curve is modeled with the function given by eq 4, where $I(E)$ is the normalized intensity of the product ion at center-of-mass collision energy E, E_T is the desired threshold energy,

$$I(E) = I_0[(E - E_T)^n/E] \tag{4}$$

I_0 is a scaling factor, and n is an adjustable parameter.[19–21] The above function is convoluted with the reactant ion kinetic energy distribution (approximated by a Gaussian function with a 2 eV lab fwhm) and a Doppler broadening function developed by Chantry to account for the random thermal motion of the neutral target,[22] and the composite function is fit to the experimental data. Optimization is carried out by an iterative procedure in which n, I_0, and E_T are varied so as to minimize the deviations between the experimental and calculated appearance curves in the steeply rising portion of the threshold region.[23] The region very near the threshold is not included in the fit because of tailing in the data attributed to translational excitation of the ions in the first quadrupole, and/or internal excitation in the reactant ions caused by collisions outside the interaction region. The CID threshold, E_T, derived in this way is considered to correspond to a *thermal* activation energy for production of room temperature (298 K) products from thermalized, room temperature reactants.[19] The error limits quoted below for the fitting parameters are standard deviations for the parameters optimized for the individual data sets. The standard deviation of E_T is taken to be a good estimate for the uncertainty in the derived thresholds.

Results and Discussion

The iron hydroxycarbonyl complex I is formed as the sole product from reactions between $HO^-(H_2O)_n$ clusters ($n = 1-4$)

(12) Laine, R. M.; Crawford, E. J. *J. Mol. Catal.* **1988**, *44*, 357–387.

(13) Lane, K. R.; Sallans, L.; Squires, R. R. *Inorg. Chem.* **1984**, *23*, 1999–2000.

(14) Graul, S. T.; Squires, R. R. *Mass Spectrom. Rev.* **1988**, *7*, 263–358.

(15) Lane, K. R.; Sallans, L.; Squires, R. R. *J. Am. Chem. Soc.* **1986**, *108*, 4368–4378. Lane, K. R.; Squires, R. R. *J. Am. Chem. Soc.* **1986**, *108*, 7187–7194.

(16) Squires, R. R. *Int. J. Mass Spectrom. Ion Processes* **1992**, *117*, 565–600.

(17) Ferguson, E. E.; Fehsenfeld, F. C.; Schmeltekopf, A. *Adv. At. Mol. Phys.* **1969**, *5*, 1–56. Smith, D.; Adams, N. C. In *Gas Phase Ion Chemistry*; Bowers, M. T., Ed.; Academic Press: New York, 1979.

(18) Ikezoe, Y.; Matsuoka, S.; Takebe, M.; Viggiano, A. *Gas Phase Ion-Molecular Reaction Rate Constants Through 1986*; Maruzen: Tokyo, 1987.

(19) Sunderlin, L. S.; Wang, D.; Squires, R. R. *J. Am. Chem. Soc.* **1992**, *114*, 2788–2796.

(20) Graul, S. T.; Squires, R. R. *J. Am. Chem. Soc.* **1990**, *112*, 2517–2529. Paulino, J. A.; Squires, R. R. *J. Am. Chem. Soc.* **1991**, *113*, 5573–5580.

(21) Rebick, C.; Levine, R. D. *J. Chem. Phys.* **1973**, *58*, 3942–3952. Sunderlin, L. S.; Armentrout, P. B. *Int. J. Mass Spec. Ion Processes* **1989**, *94*, 149–177 and references therein. Chesnavich, W. J.; Bowers, M. T. *J. Phys. Chem.* **1989**, *83*, 900–905. Gislason, E. A.; Sizun, M. *J. Phys. Chem.* **1991**, *95*, 8462–8466 and references therein.

(22) Chantry, P. J. *J. Chem. Phys.* **1971**, *55*, 2746–2759.

(23) We thank Professors P. B. Armentrout and K. M. Ervin for the CRUNCH program used for data analysis.

or $HOCO_2^-$ and $Fe(CO)_5$.[4] The ions formed through these two routes have indistinguishable CID spectra, indicating that they have the same structure. Identification of the species produced in the former reaction as the iron hydroxycarbonyl complex has been discussed previously.[4] I undergoes H/D exchange in the presence of CH_3COOH and H_2S—behavior that is inconsistent with a formate structure, $(CO)_4FeO_2CH^-$. Moreover, I is inert toward addition or substitution by *n*-donor ligands, as would be expected of a stable 18-electron metal complex, and it does not react with strongly polar molecules such as CH_3NO_2, thereby ruling out an electrostatically bound cluster. Addition of a wide variety of solvated and unsolvated nucleophilic anions to $Fe(CO)_5$ in the gas phase has been found to produce stable and relatively unreactive metal–acyl complexes $(CO)_4FeC(O)X^-$.[15] Following our original report of the observation of $(CO)_4FeCOOH^-$ in the gas phase, Ford and co-workers successfully generated and spectroscopically characterized this formerly elusive species in anhydrous, homogeneous solution.[6d]

Thermodynamics of Decarboxylation and Decarbonylation of I. Reliable heats of formation for $(CO)_4FeCOOH^-$ and its decarboxylation and decarbonylation products are necessary for determining the energetics of its unimolecular reactions. In the earlier investigation, limits on the hydroxide affinity of $Fe(CO)_5$ were inferred from the observed reactivity of I. Thus, the occurrence of reaction 3b for *n* = 4 was used to derive a lower limit of $DH[Fe(CO)_5–OH^-] \geq 53.1$ kcal/mol.[24] Bimolecular switching-type reactions were observed between other iron acylates and water. The particular reaction illustrated in eq 5 was used to infer an upper limit for $DH[Fe(CO)_5–OH^-]$ of 60.3 ± 3 kcal/mol.[24] Thus, the OH^- affinity of $Fe(CO)_5$ was bracketed between 53.1 and 60.3 kcal/mol.

$$(CO)_4FeCOF^- + H_2O \rightarrow (CO)_4FeCOOH^- + HF \quad (5)$$
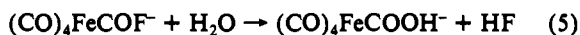
In the course of qualitative studies of the reactivity of I, we have now observed that transfer of OH^- between $Fe(CO)_5$ and SO_2 is a *reversible* reaction (eq 6). This could only be true if

$$(CO)_4FeCOOH^- + SO_2 \rightleftharpoons Fe(CO)_5 + HOSO_2^- \quad (6)$$
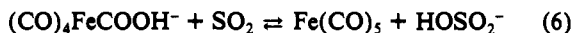
these two species have similar hydroxide affinities. Since the heat of formation of $HOSO_2^-$ (bisulfite) and the hydroxide affinity of SO_2 have been recently measured,[16] the measured equilibrium constant for OH^- exchange can be used to determine the hydroxide affinity of $Fe(CO)_5$, and therefore $\Delta H_f[(CO)_4FeCOOH^-]$. The kinetics of the reaction of $(CO)_4FeCOOH^-$ with SO_2, and the reaction of $HOSO_2^-$ with $Fe(CO)_5$, were therefore measured at room temperature using standard flowing afterglow techniques.[14,17] The primary products observed are listed in reactions 7 and 8.

$$(CO)_4FeCOOH^- + SO_2 \longrightarrow \begin{cases} Fe(CO)_5 + HOSO_2^- & (7a) \\ (CO)_4Fe(SO_2)H^- + CO_2 & (7b) \end{cases}$$

$$Fe(CO)_5 + HOSO_2^- \longrightarrow \begin{cases} (CO)_4FeCOOH^- + SO_2 & (8a) \\ (CO)_4Fe(SO_2)H^- + CO_2 & (8b) \end{cases}$$

In addition to hydroxide exchange, formation of an abundant side product with *m/z* 233 is observed in both reactions (eqs 7b and 8b). This formally corresponds to the displacement of CO_2 by SO_2 in I, giving a product with the constitution $[(CO)_4Fe(SO_2)(H)^-]$ (II). To our knowledge this organometallic reaction is unprecedented in solution. Plausible structures for II include the sulfinic acid IIa, the *S*-sulfinate IIb, and the *O*-sulfinate IIc.[25]
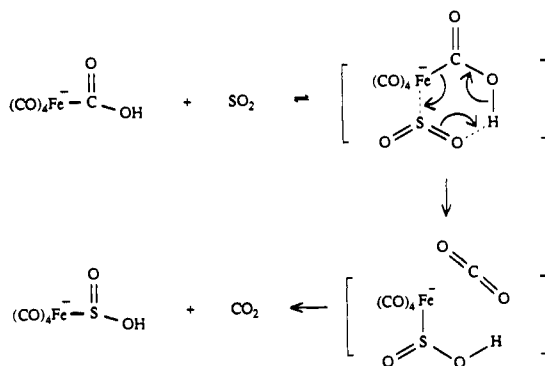
Some indirect evidence for the structure of II can be obtained from its reactivity. II does not react with NO, nor does it appear to undergo secondary reactions with SO_2. This suggests that II is a coordinatively saturated (18-electron) species, since NO and SO_2 generally react by addition and substitution with unsaturated organometallic anions in the gas phase.[2,26] Hydrogen/deuterium exchange is observed in the reaction of II with CH_3COOD, but not with D_2O or CH_3OD. Identical behavior was previously observed for $(CO)_4FeCOOH^-$, which suggests (but does not require) that II also possesses an O–H bond. H/D exchange with structures IIb and IIc would most likely lead to isomerization of the sulfur-containing ligand, since both structures possess an S–H bond, but deuteration at either the metal or oxygen is obligatory with IIb and IIc. CID of II results in formation of $Fe(CO)_4^- +$ [S, 2O, H], reaction 9, with a measured threshold energy of 24.9 $\pm$ 2.3 kcal/mol. Identical fragment ion appearance curves and

$$(CO)_4Fe[SO_2]H^- \xrightarrow{CID} Fe(CO)_4^- + [SOOH] \quad (9)$$
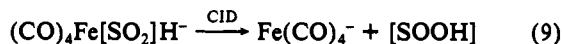
associated thresholds are obtained for II formed by either reaction 7b or 8b and for deuterated II produced by H/D exchange. These results are most consistent with structure IIa, since H/D exchange would not isomerize the sulfinic acid ligand.

A plausible mechanism for the formation of IIa involves initial formation of an $(CO)_4FeCOOH^-–SO_2$ ion–dipole complex, followed by either a stepwise or a concerted expulsion of CO_2 with accompanying formation of Fe–S and SO_2–H bonds (Scheme II). The exact sequence of the bond forming and breaking in this mechanism is a matter for speculation. It is noteworthy that the methyl analog of I, $(CO)_4FeCOOCH_3^-$, reacts with SO_2 only by methoxide transfer, reaction 10.[27] No formation of $(CO)_4FeS$-

$$(CO)_4FeCOOCH_3^- + SO_2 \rightarrow Fe(CO)_5 + CH_3OSO_2^- \quad (10)$$
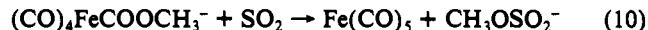
$OOCH_3^-$, the methyl analog of IIa, is observed. This is consistent with an acid–base character for the putative SO–H bond formation step in reaction 7b.

The rate constants for reactions 7 and 8, measured as described above, are $(1.9 \pm 0.6) \times 10^{-10}$ cm³/s and $(1.6 \pm 0.5) \times 10^{-10}$ cm³/s, respectively. The branching ratio for reactions 7a and 7b is 55:45, while for reactions 8a and 8b the branching ratio is 25:75. The ratio of the rate constants for reactions 7a and 8a gives the equilibrium constant for reaction 6, $K(6) = 2.6$. The competing side reactions 7b and 8b could perturb the rates for reactions 7a and 8a, and therefore the calculated equilibrium constant, by a factor of up to 4 (the ratio of the total rate for reaction 8 to the partial rate for reaction 8a).[28] On the basis of these consider-
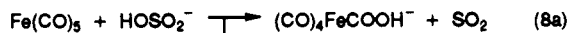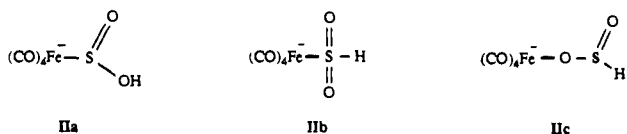
Scheme II

(24) Lane, K. R.; Sallans, L.; Squires, R. R. *J. Am. Chem. Soc.* **1985**, *107*, 5369–5375.

(25) Ryan, R. R.; Kubas, G. J.; Moody, D. C.; Eller, P. G. *Struct. Bonding (Berlin)* **1981**, *46*, 47–100.

(26) See for example: McDonald, R. N.; Schell, P. L. *Organometallics* **1988**, *7*, 1806–1820, 1820–1827.

(27) This reaction does not appear to go to completion with increasing concentrations of SO_2, suggesting that back reaction is probably occurring. This would imply that the methoxide transfer in reaction 10 is near thermoneutral. Since the hydroxide affinities of $Fe(CO)_5$ and SO_2 are nearly identical, it is reasonable that the methoxide affinities should also be similar.

(28) Bohme, D. K.; Hemsworth, R. S.; Rundle, H. W.; Schiff, H. I. *J. Chem. Phys.* **1973**, *58*, 3504–3518. Davidson, W. R.; Bowers, M. T.; Su, T.; Aue, D. H. *Int. J. Mass Spectrom. Ion Phys.* **1977**, *24*, 83–105.

**Table I.** Supplemental and Measured Thermochemistry[a]

species	ΔH_f (kcal/mol)	species	ΔH_f (kcal/mol)
CO	-26.42	OH⁻	-32.8 ± 0.1[c]
CO₂	-94.05	(CO)₄FeH₂	-130.5 ± 3.5[d]
Fe(CO)₅	-173 ± 2	(CO)₄FeH⁻	-177 ± 6[d]
Fe(CO)₄	-104.5 ± 2.8[b]	(CO)₄FeOH⁻	-219 ± 6[d]
H₂O	-57.80	(CO)₄FeCOOH⁻	-267 ± 4[d]
H⁺	365.7		

[a] Unless otherwise noted, data are from the following: Lias, S. G.; Bartmess, J. E.; Liebman, J. F.; Holmes, J. L.; Levin, R. D.; Mallard, W. G. *J. Phys. Chem. Ref. Data* **1988**, *17*, Suppl. 1. All values at 298 K. [b] Reference 30. [c] Bartmess, J, E. Negative Ion Energetics Database, Version 2.90, Standard Reference Data, NIST, Gaithersburg, MD 20899 (1989). [d] See text.

ations, we assign the free energy change for reaction 6, $\Delta G(6)$, to be -0.6 ± 1.0 kcal/mol.

Insufficient information is available to determine precisely the entropy change for reaction 6. However, most factors should cancel except for changes in the translational entropy, rotational symmetry, and internal rotors of the species involved. The rotational symmetries of the relevant species are as follows: (CO)₄FeCOOH⁻, $\sigma = 1$; SO₂, $\sigma = 2$; Fe(CO)₅, $\sigma = 6$; HOSO₂⁻, $\sigma = 1$. The rotational symmetry contribution to ΔS for reaction 6 is therefore $R \ln (2/6) = -2.2$ eu. The translational entropy contribution to reaction 6 is 0.6 eu. The overall number of rotations is conserved in the hydroxide exchange reaction. However, there are internal rotors in both (CO)₄FeCOOH⁻ and HOSO₂⁻ which may have a significant effect on ΔS for the reaction. Given the current lack of detailed calculations or spectroscopy on the species involved, we assume the effects of internal rotations cancel. The error involved in this assumption should be at most about 2 kcal/mol at 298 K. Thus, given the assumptions listed above, $T\Delta S$ for reaction 6 is -0.5 ± 2 kcal/mol. Since $\Delta G = -0.6 ± 1.0$ kcal/mol, $\Delta H = -1.1 ± 2.2$ kcal/mol. This latter value can be combined with the recently measured heterolytic bond strength DH[SO₂–OH⁻] = 61.9 ± 2.5 kcal/mol[16] to give DH[Fe(CO)₅–OH⁻] = 60.8 ± 3.4 kcal/mol. This result is consistent with the limits 53.1 kcal/mol ≤ DH[Fe(CO)₅–OH⁻] ≤ 60.3 ± 3 kcal/mol discussed above.[4,24] The derived bond strength can be combined with ΔH_f[Fe(CO)₅] = -173 ± 2 kcal/mol and ΔH_f[OH⁻] = -32.7 kcal/mol from Table I to give ΔH_f[(CO)₄FeCOOH⁻] = -267 ± 4 kcal/mol.
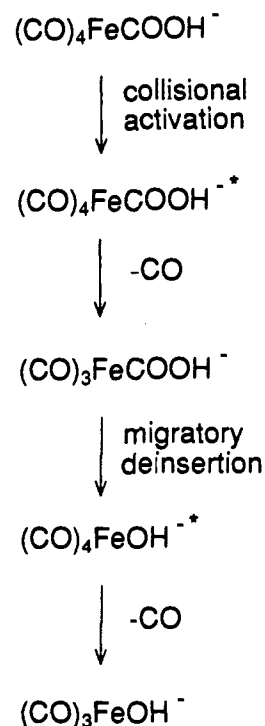
In order to determine the overall energetics of decarboxylation of (CO)₄FeCOOH⁻, the heat of formation of the iron hydride product, (CO)₄FeH⁻, is required. The enthalpy of reaction 11 in solution has been measured to be 26 ± 2 kcal/mol.[8,29] We assume that this value is also applicable to the gas phase, noting

$$(CO)_4FeH_2 \rightarrow Fe(CO)_4 + H_2 \qquad (11)$$

$$Fe(CO)_5 \rightarrow Fe(CO)_4 + CO \qquad (12)$$
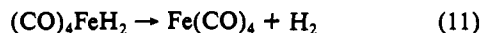
that the gas phase and solution enthalpies of activation for the analogous reaction 12, 42.1 ± 2 kcal/mol[30] and 42.5 ± 1.2 kcal/mol,[31] are essentially identical. This value can be combined with data in Table I to give ΔH_f[(CO)₄FeH₂] = -130.5 ± 3.5 kcal/mol. Combining this value with the recently reported gas-phase acidity of [(CO)₄FeH₂], 319 ± 5 kcal/mol,[29] gives ΔH_f[(CO)₄FeH⁻] = -177 ± 6 kcal/mol. Therefore, the enthalpy change for decarboxylation of (CO)₄FeCOOH⁻ in the gas phase, reaction 1, is -4 ± 7 kcal/mol.

Decarbonylation of (CO)₄FeCOOH⁻ without rearrangement gives the 16-electron complex (CO)₃FeCOOH⁻. The hydroxide ligand can undergo migratory deinsertion sequentially or simultaneously to the empty site on the iron, giving the 18-electron complex (CO)₄FeOH⁻, where OH⁻ is a two-electron donor.[15] At this point the complex may have enough internal energy for

(29) Stevens Miller, A. E.; Beauchamp, J. L. *J. Am. Chem. Soc.* **1991**, *113*, 8765–8770.

(30) Lewis, K. E.; Golden, D. M.; Smith, G. P. *J. Am. Chem. Soc.* **1984**, *106*, 3905–3912.

(31) Siefert, E. E.; Angelici, R. J. *Organomet. Chem.* **1967**, *8*, 374–376.

Scheme III

$(CO)_4FeCOOH^-$

↓ collisional activation

$(CO)_4FeCOOH^{-\bullet}$

↓ -CO

$(CO)_3FeCOOH^-$

↓ migratory deinsertion

$(CO)_4FeOH^{-\bullet}$

↓ -CO

$(CO)_3FeOH^-$

Table II. Anion Affinities of Fe(CO)₄[a]

X⁻	PA(X⁻)	DH[(CO)₄Fe–X⁻]
⁻COCH₃	391.0 ± 2.6	83[b]
⁻COOH	382[f]	81[c]
⁻COOCH₃	391.8 ± 0.9[d]	88[b]
⁻CHO	393.4 ± 0.7	90 ± 5[e]
⁻OH	390.7	

[a] All data in kcal/mol. Unless otherwise noted, proton affinities are from the following: Lias, S. G.; Bartmess, J. E.; Liebman, J. F.; Holmes, J. L.; Levin, R. D.; Mallard, W. G. *J. Phys. Chem. Ref. Data* **1988**, *17*, Suppl. 1. [b] Derived using eq 14 and data in ref 24. [c] Derived using eq 14 and DH[(CO)₅Fe–OH⁻] from the present work. [d] Bartmess, J. E. Negative Ion Energetics Database, Version 2.90, Standard Reference Data, NIST, Gaithersburg, MD 20899 (1989). DePuy, C. H.; Grabowski, J. J.; Bierbaum, V. M.; Ingemann, S.; Nibbering, N. M. M. *J. Am. Chem. Soc.* **1985**, *107*, 1093–1098. [e] Lane, K. R.; Squires, R. R. *Polyhedron* **1988**, *7*, 1609–1618. [f] Sheldon, J. C.; Bowie, J. H. *J. Am. Chem. Soc.* **1990**, *112*, 2424–2425.

dissociation of a second CO ligand to give (CO)₃FeOH⁻, where OH⁻ can act as a four-electron donor in an 18-electron complex. This mechanism, illustrated in Scheme III, has been demonstrated and discussed in detail previously.[15]

The heat of formation of (CO)₄FeOH⁻ was estimated previously using a correlation between the proton affinities of anions, PA(X⁻), and the binding enthalpies of the anions to Fe(CO)₄, DH[(CO)₄Fe–X⁻]. This correlation is analogous to the one proposed for PA(X⁻) and DH[Fe(CO)₅–X⁻].[24] Additional values for DH[(CO)₄Fe–X⁻] (iron tetracarbonyl affinities) are now available through use of eq 13, which, after rearrangement and substitution of DH[(CO)₄Fe–CO] = 42.1 ± 2 kcal/mol,[30] gives eq 14. The relevant data are given in Table II. The anions listed in Table

$$DH[(CO)_4Fe–COX^-] + DH(CO–X^-) =$$
$$DH[Fe(CO)_5–X^-] + DH[(CO)_4Fe–CO] \quad (13)$$

$$DH[(CO)_4Fe–COX^-] =$$
$$DH[Fe(CO)_5–X^-] + 42.1 ± 2 \text{ kcal/mol} - DH(CO–X^-)$$
$$(14)$$

II have similar proton affinities to that of OH⁻, and their Fe(CO)₄ affinities all lie in the 81–90 kcal/mol range. We therefore expect the Fe(CO)₄ affinity of OH⁻ to be in this range as well, and estimate DH[(CO)₄Fe–OH⁻] = 85 ± 5 kcal/mol. From this we

Figure 1. Appearance curves for low energy products from CID of $(CO)_4FeCOOH^-$ as a function of kinetic energy in the center-of-mass frame. The solid lines are model appearance curves calculated using eq 4 and convoluted as discussed in the text.

Table III. Fitting Parameters

reaction no.	threshold, E_t (eV)	n (eq 4)	σ_{max} (Å^2)
9	1.08 ± 0.10	1.89 ± 0.13	5
15	0.93 ± 0.17	1.85 ± 0.14	3.5
16	1.31 ± 0.12	1.79 ± 0.12	18
17	3.25 ± 0.19	1.58 ± 0.28	4.0
18	4.64 ± 0.31	2.07 ± 0.20	0.9
19	0.82 ± 0.14	1.72 ± 0.13	0.7
20	≈4		0.1
21	4.0 ± 0.6	1.6 ± 0.2	1.4
22	5.41 ± 0.44	1.77 ± 0.09	0.5
23	≈6		0.03

derive $\Delta H_f[(CO)_4FeOH^-] = -222 \pm 6$ kcal/mol, which implies that decarbonylation of $(CO)_4FeCOOH^-$ is endothermic by 18 ± 7 kcal/mol.

Collision-Induced Dissociation of $(CO)_4FeCOOH^-$. Figures 1 and 2 illustrate the energy-dependent cross sections for the major metal-containing fragment ions observed from CID of **I**. The products observed are shown in reactions 15–23 and correspond to loss of CO, CO_2, and [COOH],[32] all accompanied by loss of

$(CO)_4FeCOOH^- \xrightarrow{\text{Ar CID}}$

$\longrightarrow (CO)_4FeOH^- + CO$	(15)
$\longrightarrow (CO)_3FeOH^- + 2CO$	(16)
$\longrightarrow (CO)_2FeOH^- + 3CO$	(17)
$\longrightarrow (CO)FeOH^- + 4CO$	(18)
$\longrightarrow (CO)_4FeH^- + CO_2$	(19)
$\longrightarrow (CO)_3FeH^- + CO_2 + CO$	(20)
$\longrightarrow Fe(CO)_4^- + [CO_2H]$	(21)
$\longrightarrow Fe(CO)_3^- + [CO_2H] + CO$	(22)
$\longrightarrow Fe(CO)_2^- + [CO_2H] + 2CO$	(23)

further CO ligands at higher energies. Cross sections for the lowest-energy reactions, processes 15, 16, and 19, are plotted as a function of kinetic energy in Figure 1, and cross sections for

---

(32) Loss of 45 amu (C, 2O, H) from the reactant ion reasonably corresponds to COOH, CO + OH, or CO_2 + H. Since loss of OH or OH⁻ is not observed, loss of CO + OH is unlikely. Loss of COOH (hydroxyformyl radical) is the lower energy pathway of the remaining two possibilities, and is therefore presumed to be the main reaction.

Figure 2. Appearance curves for high-energy products from CID of $(CO)_4FeCOOH^-$ as a function of kinetic energy in the center-of-mass frame. The solid lines are model appearance curves calculated using eq 4 and convoluted as discussed in the text.

processes 17, 18, and 21 are shown in Figure 2. The maximum absolute cross sections for these reactions are listed in Table III. At higher energies, losses of progressively more ligands become the major product channels. No other products are observed within the sensitivity of the detector, although electron detachment is a possibility that would not be detected with our instrument.

Base catalysis has been invoked for decarboxylation in solution.[8] To test whether decarboxylation can be catalyzed by a neutral base in the gas phase, the reaction of $(CO)_4FeCOOH^-$ with NH_3 was examined at both thermal and elevated kinetic energies. It was previously observed that base-catalyzed decarboxylation does not occur during reaction of **I** with either NH_3 or $(CH_3)_2NH$ in the flow tube at thermal energies.[4] In contrast, $Fe(CO)_5$ is observed to react with the ammonia cluster ion $OH^-(NH_3)$ to produce $(CO)_4FeH^-$ as a minor product.[15] In this reaction, the NH_3 is apparently able to catalyze decarboxylation within the initially formed, energy-rich $[(CO)_4FeCOOH^--NH_3]$ intermediate. We have attempted to model this process by examining the reaction of **I** with NH_3 in the triple quadrupole. In principle, the barrier for base-induced decarboxylation could be overcome with elevated collision energies. However, no measurable shift in the threshold for decarboxylation of **I** is observed with ammonia as the target gas compared to argon as the target gas, indicating that ammonia does not lower the barrier for loss of CO_2 in the gas phase. Also, $(CO)_4FeCOOD^-$ does not exchange with NH_3 during decarboxylation in the triple quadrupole to form $(CO)_4-FeH^-$, as would be expected if base catalysis involved a concerted 6-center reaction.[15]

The optimized fitting parameters for eq 4 found by modeling the appearance curves for reactions 15–23 are listed in Table III, and the corresponding fits are shown in Figures 1 and 2. For $(CO)_4FeCOOH^-$, the thresholds for loss of CO and CO_2 are both near 1 eV, while the threshold for loss of 2CO is only ca. 0.4 eV higher. Loss of [COOH] has a much higher threshold of approximately 4 eV.

The thresholds derived for reactions 18 and 20–23 are relatively uncertain because of small cross sections that give low signal/noise ratios, and/or because of other reactions that have much larger cross sections. This can cause competitive shifts that affect the shape of the appearance curves (typically causing them to rise slowly from the threshold) and make determining the proper fitting parameters problematical.[33]

The thresholds for reactions 15–23 are measurements of the activation energies for these dissociations. An important question is whether any of these reactions have nonzero reverse activation energies, i.e. whether the reaction thresholds correspond to the

---

(33) Lifschitz, C.; Long, F. A. *J. Chem. Phys.* **1964**, *41*, 2468–2471. Schultz, R. H.; Crellin, K. C.; Armentrout, P. B. *J. Am. Chem. Soc.* **1991**, *113*, 8590–8601.

342 *J. Am. Chem. Soc., Vol. 115, No. 1, 1993*

Sunderlin and Squires

overall reaction endothermicity or to a reaction barrier. The discrepancy between the known exothermicity for reaction 19 (-4 ± 7 kcal/mol) and the observed threshold energy (18.9 ± 3.2 kcal/mol) clearly indicates that the measured threshold corresponds to a barrier rather than to the overall reaction energetics. The high barrier explains why I is stable in the gas phase with respect to decarboxylation, and can be plausibly attributed to the concerted β-hydrogen shift that is necessary for CO_2 loss to occur.

The barrier to decarboxylation indicates that there is also a substantial barrier to insertion of CO_2 into the Fe–H bond of $(CO)_4FeH^-$ to form I. Although the insertion of CO_2 into metal–hydrogen bonds is common, the observed product is essentially always a formate rather than a hydroxycarbonyl species.[34] This can be attributed to both the generally greater thermodynamic stability of formates compared to hydroxycarbonyls and favorable dipole interactions between a typically M^+-H^- polarized metal–hydrogen bond and the O^--C^+ oxygen–carbon bond in CO_2.

The measured threshold for decarbonylation (reaction 15) is 21.4 ± 3.9 kcal/mol, much lower than the energy required for decarbonylation of $Fe(CO)_5$, 41.5 kcal/mol.[30] This reflects the strong CO-labilizing influence[35] of the acyl ligand in I, and/or the energetics of migration of the hydroxide ligand to the metal. The reaction apparently proceeds at or near the thermochemical limit since the endothermicity estimated above, 18 ± 7 kcal/mol, is nearly the same as the reaction threshold. This may suggest that the OH⁻ ligand migration is synchronous with the dissociation of a carbonyl ligand. An analogous mechanism for unimolecular decarbonylation of $(CO)_3Fe(\eta^2\text{-butadiene})^-$ in the gas phase was recently proposed by Dillow and Kebarle[36] (eq 24). In this reaction, a CO ligand is replaced by an alkene group in the ligand

$$(CO)_3Fe(\eta^2\text{-butadiene})^- \rightarrow (CO)_2Fe(\eta^4\text{-butadiene})^- + CO$$
$$(24)$$
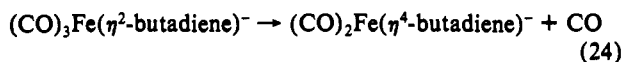
sphere of the iron atom. Reaction 24 is reported to be endothermic by 20 kcal/mol and to have a negligible reverse activation barrier, comparable to what is found for reaction 15. Taking the excess energy barrier for reaction 15 to be negligible gives ΔH_f $[(CO)_4FeOH^-]$ = -219 ± 6 kcal/mol; -219 ± 6 kcal/mol, in good agreement with the value derived from the estimated OH⁻ affinity of $Fe(CO)_4$. A barrier would mean that the heat of formation is somewhat lower.

The energy cost for dissociation of a second CO ligand from I is the difference between the endothermicities for reactions 15 and 16, 8.8 ± 4.6 kcal/mol. This unusually low value can be attributed to the CO-labilizing effect of the OH⁻ in $(CO)_4FeOH^-$, in which loss of a CO ligand allows π-donation from the OH⁻ ligand to the metal.[37] Further losses of CO have correspondingly higher thresholds consistent with the Fe–CO bond strengths in $Fe(CO)_4^-$.[19]

For some CID processes, it is possible to examine the reverse, bimolecular addition reaction to determine whether a significant reverse activation energy exists. A reaction that proceeds rapidly at room temperature cannot have a significant barrier, while a reaction that does not proceed at a measurable rate may have a barrier or other kinetic constraints. Addition of CO to the hydride $(CO)_3FeH^-$ proceeds rapidly in the flow tube,[38] as expected for a 16-electron species. In contrast, CO does not add to either $(CO)_3FeOH^-$ or $(CO)_4FeOH^-$ under flowing afterglow conditions. This suggests that these anions incorporate 18-electron metal centers that do not easily bind an additional CO ligand without
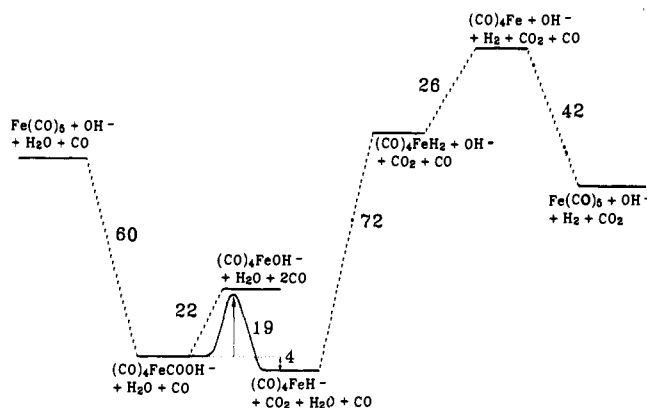

Figure 3. Thermochemical profile for the model $Fe(CO)_5$-catalyzed water-gas shift reaction in the gas phase (enthalpies in kcal/mol).

significant rearrangement (i.e. migratory insertion). For (C-O)$_4$FeOH⁻, although the thermochemistry discussed above suggests there is no large barrier, the lack of CO addition indicates that a small barrier or a kinetic bottleneck must exist for decarbonylation of I. In the case of $(CO)_3FeOH^-$, CO addition may be disfavored because of a strong π-interaction of the OH⁻ ligand with iron (vide supra), effectively saturating the metal center.

Cross Sections. Analysis of the reaction cross sections can provide insight into the dissociation mechanisms. Just as a reaction threshold corresponds to the activation energy for a particular process, the maximum reaction cross section (σ_{max}) can be compared to the Arrhenius A factor for a reaction. At a given energy, reactions that have large cross sections are less constrained by energetic or dynamical effects than reactions that have small cross sections. In general, higher energy processes have lower CID cross sections. However, the unimolecular decomposition of I is atypical in that the largest cross section belongs to reaction 16, which has the third highest threshold (Table III). Furthermore, although reactions 15 and 19 have similar thresholds, reaction 15 is significantly more probable than reaction 19. Useful data for comparison to the present results are the cross sections for CID of $Fe(CO)_n^-$, n = 2–4.[19] Loss of a single carbonyl ligand from these ions has a maximum cross section of 7–16 Å². Cross sections for loss of two or three carbonyl ligands are smaller by factors of 5–35. All of these reactions are simple bond cleavages. In contrast, the maximum cross sections for loss of one, two, and three carbonyl ligands from I are in the approximate ratio 1:5:1. Compared to the $Fe(CO)_4^-$ system, loss of a single carbonyl ligand is disfavored, while loss of two carbonyl ligands is favored. The small difference between the thresholds for loss of one and two carbonyl ligands from I means that only a relatively narrow range of energy transfer to $(CO)_4FeCOOH^-$ will typically result in loss of exactly one CO ligand, leading to a low cross section for that process. The overall total CID cross section for I is similar to that for the simple metal carbonyl anions. Loss of three or four carbonyl ligands from I shows successively smaller cross sections, although the relative decline is somewhat less than for $Fe(CO)_4^-$.

Loss of CO_2 has a very small maximum cross section, and the cross section begins to decline at relatively low energy. This explains why this dissociation reaction was not detected in the earlier study of this system.[4] The prototype instrument used previously suffered from low sensitivity, and the high target pressures and collision energies that were employed suppressed the appearance of the CO_2-loss channel. Below 2 eV, loss of CO is a factor of 5 more efficient than loss of CO_2. This effect is even more pronounced when the cross sections for further losses of CO ligands (reactions 16–18) are added to the cross section for reaction 15. The difference is not due to energetics since the two reactions have nearly identical thresholds. Reaction 19 must therefore have a tighter transition state than reaction 15. This corresponds to a concerted mechanism for reaction 19. Very little loss of CO_2 + nCO is observed. This can be understood by noting that if sufficient energy is deposited in $(CO)_4FeCOOH^-$ to remove both a CO_2 and one or more CO ligands, then the kinetically favored

(34) Darensbourg, D. J.; Kudaroski, R. A. *Adv. Organomet. Chem.* **1983**, *22*, 129–168. Braunstein, P.; Matt, D.; Nobel, D. *Chem. Rev.* **1988**, *88*, 747–764. Sakaki, S.; Ohkubo, K. *Inorg. Chem.* **1989**, *28*, 2583–2590. Koga, N.; Morokuma, K. In *Transition Metal Hydrides*; Dedieu, A., Ed.; VCH: New York, 1992.

(35) Collman, J. P.; Hegedus, L. S.; Norton, J. R.; Finke, R. G. *Principles and Applications of Organotransition Metal Chemistry*; University Science Books: Mill Valley, CA, 1987.

(36) Dillow, G. W.; Kebarle, P. *J. Am. Chem. Soc.* **1992**, *114*, 5742–5747.

(37) Lichtenberger, D. L.; Brown, T. L. *J. Am. Chem. Soc.* **1978**, *100*, 366–373. Atwood, J. D.; Brown, T. L. *J. Am. Chem. Soc.* **1976**, *98*, 3155–3159, 3160–3166.

(38) Lane, K. R. Ph.D. Thesis, Purdue University, 1986.

CO-dissociation channel will dominate.[39] Loss of [COOH] has a relatively low cross section because of the relatively high energy requirement.

Implications for the Fe(CO)₅-Catalyzed WGS Reaction. Given the thermochemical information accumulated above, we can now construct a relatively complete energy profile for the Fe(CO)₅-catalyzed WGS reaction in the gas phase for comparison to solution-phase results. This is illustrated in Figure 3. In the gas phase, the initial step of addition of OH⁻ to Fe(CO)₅ is highly exothermic. This step is slower in solution because OH⁻ is more effectively solvated than the bulkier (CO)₄FeCOOH⁻.[6d] Both decarboxylation and decarbonylation of I have similar barriers or endothermicities. In solution, decarboxylation is generally rapid,[10,11] which suggests that the barrier for decarboxylation is lowered by solvation. The barrier for decarbonylation may be low, but the high pressure of CO generally used in condensed-phase experiments prevents observation of decarbonylation products by shifting the equilibrium in favor of back reaction. Decarbonylation products in the form of polynuclear iron carbonyls are observed in the absence of CO.[8] Next, proton transfer from water to (CO)₄FeH⁻ is strongly endothermic in the gas phase, since (C-O)₄FeH₂ is a very weak acid.[29] However, this step can occur in solution because the pK_a of (CO)₄FeH₂ is 5.9 in 70% methanol–water solution.[8] Nevertheless, the rate of reaction will be slow in basic solutions, as has been reported previously. Loss of H₂ followed by addition of CO to reform Fe(CO)₅ is exothermic in the gas phase, and rapid in solution.

Ford and Rokicki have noted that an open coordination site on the metal and a lack of steric hindrance are necessary for the concerted elimination of CO₂ from metal hydroxycarbonyls in solution.[5] Both of these criteria are met in the present system. Thus, the barrier to reaction in the present system is likely to be a lower limit to the barrier for similar systems where these criteria are not met. The activation energy for the Fe(CO)₅-catalyzed WGS reaction in solution has been measured to be 22 kcal/mol,[10,11] which is quite close to the gas-phase decarboxylation activation energy of 19 kcal/mol. However, the fact that Fe(CO)₅ and (CO)₄FeH⁻ but not (CO)₄FeCOOH⁻ are observed in active catalytic solutions[10,11] suggests that decarboxylation is not the rate-limiting step in solution.

The WGS catalysis by group 6 metals apparently involves formation of formate complexes.[11,40–42] Darensbourg et al.[41] have recently noted that loss of CO from (CO)₅Cr(O₂CH)⁻ has an activation enthalpy of 18.9 ± 0.7 kcal/mol. This barrier is quite close to that measured for CO loss in the present system. Darensbourg et al. propose that CO loss generally precedes CO₂ loss. Dissociation of CO allows hydride migration to the open bonding site and loss of CO₂, after which CO reassociates with the metal. In the gas phase, the fact that [CO + CO₂] loss is not a significant process at any energy argues strongly against such a mechanism in the iron hydroxycarbonyl system.

The primary evidence in favor of the base-catalyzed mechanism is the fact that the turnover rate for the overall WGS reaction (Scheme I) is proportional to base concentration in the 1.2–175 mM range.[8] This is consistent with the first step of reaction 2; however, it is also consistent with reaction 1 if the rate-limiting step in Scheme I is formation of (CO)₄FeCOOH⁻.[6d] Since (CO)₄FeCOOH⁻ is not observed in catalytic solutions, this is certainly feasible. Although formation of I is rapid in the gas phase, solvation in solution would conceivably slow the reaction.[6d] Comprehensive kinetics measurements in tetrahydrofuran/methanol/water solutions are consistent with a direct decarboxylation mechanism, but not with base catalysis.[6d] The present study supports the conclusion that base catalysis is not necessary for decarboxylation.

Summary. The heat of formation of (CO)₄FeCOOH⁻ has been determined by measurement of the equilibrium constant for the near-thermoneutral OH⁻ transfer to SO₂. An unusual exchange of SO₂ for CO₂ is also observed in the reaction of (CO)₄FeCOOH⁻ with SO₂. The heats of formation of (CO)₄FeOH⁻ and (CO)₄FeH⁻ are also derived from data in the literature. Loss of CO₂ from (CO)₄FeCOOH⁻ is shown to occur in the gas phase without base catalysis. However, the reaction has a significant barrier (18.9 ± 3.2 kcal/mol) and is kinetically disfavored compared to competing CO ligand dissociation reactions. Decarbonylation has an activation energy of 21.4 ± 3.9 kcal/mol, a value that corresponds, within error, to the endothermicity of the reaction.

(39) Cooks, R. G. In *Collision Spectroscopy*; Cooks, R. G. Ed.; Plenum: New York, 1978.

(40) Slegeir, W. A.; Sapienza, R. S.; Rayford, R.; Lam, L. *Organometallics* **1982**, *1*, 1728.

(41) Darensbourg, D. J.; Wiegriffe, H. P.; Wiegriffe, P. W. *J. Am. Chem. Soc.* **1990**, *112*, 9252–9257. Darensbourg, D. J.; Darensbourg, M. Y.; Burch, R. R.; Froelich, J. A.; Incorvia, M. J. *Adv. Chem. Ser.* **1978**, *173*, 106–120.

(42) Weiller, B. H.; Liu, J. P.; Grant, E. R. *J. Am. Chem. Soc.* **1985**, *107*, 1595–1604.